AGU100 ADVANCING EARTH AND SPACE SCIENCE

Geochemistry, Geophysics, Geosystems

RESEARCH ARTICLE

10.1029/2018GC007585

Key Points:
- We present a Bayesian approach for the inversion of geodetic data and demonstrate successful applications to synthetic and real data
- Our approach allows rapid estimates of source parameters and uncertainties and is well suited for rapid-response and operational settings
- We have implemented our approach in a MATLAB®-based software package (GBIS) that is made freely available to the scientific community

Correspondence to:
M. Bagnardi,
marco.bagnardi@jpl.nasa.gov

Citation:
Bagnardi, M., & Hooper, A. (2018). Inversion of surface deformation data for rapid estimates of source parameters and uncertainties: A Bayesian approach. *Geochemistry, Geophysics, Geosystems*, *19*, 2194–2211. https://doi.org/10.1029/2018GC007585

Received 30 MAR 2018
Accepted 14 JUN 2018
Accepted article online 27 JUN 2018
Published online 27 JUL 2018

The copyright line for this article was changed on 23 MAR 2020 after original online publication.

Inversion of Surface Deformation Data for Rapid Estimates of Source Parameters and Uncertainties: A Bayesian Approach

Marco Bagnardi[1,2] **and Andrew Hooper**[1]

[1]COMET, School of Earth and Environment, University of Leeds, Leeds, UK, [2]Now at Jet Propulsion Laboratory, California Institute of Technology, Pasadena, CA, USA

Abstract New satellite missions (e.g., the European Space Agency's Sentinel-1 constellation), advances in data downlinking, and rapid product generation now provide us with the ability to access space-geodetic data within hours of their acquisition. To truly take advantage of this opportunity, we need to be able to interpret geodetic data in a prompt and robust manner. Here we present a Bayesian approach for the inversion of multiple geodetic data sets that allows a rapid characterization of posterior probability density functions (PDFs) of source model parameters. The inversion algorithm efficiently samples posterior PDFs through a Markov chain Monte Carlo method, incorporating the Metropolis-Hastings algorithm, with automatic step size selection. We apply our approach to synthetic geodetic data simulating deformation of magmatic origin and demonstrate its ability to retrieve known source parameters. We also apply the inversion algorithm to interferometric synthetic aperture radar data measuring co-seismic displacements for a thrust-faulting earthquake (2015 M_w 6.4 Pishan earthquake, China) and retrieve optimal source parameters and associated uncertainties. Given its robustness and rapidity in estimating deformation source parameters and uncertainties, our Bayesian framework is capable of taking advantage of real-time geodetic measurements. Thus, our approach can be applied to geodetic data to study magmatic, tectonic, and other geophysical processes, especially in rapid-response operational settings (e.g., volcano observatories). Our algorithm is fully implemented in a MATLAB®-based software package (Geodetic Bayesian Inversion Software) that we make freely available to the scientific community.

1. Introduction

Geodetic observational data, most commonly global navigation satellite system (GNSS) and interferometric synthetic aperture radar (InSAR) measurements, are regularly used to infer information about sources of surface displacements and to understand the underlying processes. With these aims, inverse problem theory has been applied to geodetic data to study magmatic systems (Pinel et al., 2014, and references therein), the earthquake cycle (Elliott et al., 2016, and references therein), and many other geophysical phenomena that cause deformation of the Earth's interior and surface such as the response to ice load changes, changes in aquifer storage, and geothermal exploitation (e.g., Auriac et al., 2014; Juncu et al., 2017; Samsonov et al., 2014). However, many commonly employed inversion approaches aim at solely determining an optimal set of source parameters—for example, the weighted least-squares "best-fitting" model—by solving an optimization problem that minimizes the weighted misfit between measured and simulated surface displacements. Among these, the most commonly used methods are simulated annealing (e.g., Cervelli et al., 2001) and genetic algorithm (e.g., Currenti et al., 2005). These have shown to be successful in solving a variety of optimization problems to study different geophysical problems (Sambridge & Mosegaard, 2002), and a detailed analysis of these methodologies, applied to the inversion of InSAR data, is presented by Shirzaei and Walter (2009). Direct-search methods (e.g., simulated annealing and genetic algorithm) do not fully and appropriately characterize uncertainties associated with the source parameter estimates, with the risk that results can be inadequately interpreted. In fact, it is common that a wide range of model parameter values can adequately explain the observations, and it is therefore fundamental to know the credible interval of such values, especially if interpretations are used for the assessment and mitigation of natural hazards or in operational settings (e.g., volcano observatories).

The application of a Bayesian approach when inverting geodetic data (e.g., Anderson & Segall, 2013; Fukuda & Johnson, 2010; Hooper et al., 2013; Jolivet et al., 2015; Minson et al., 2013) allows the characterization of posterior probability density functions (PDFs) of source parameters, which are formulated by taking into

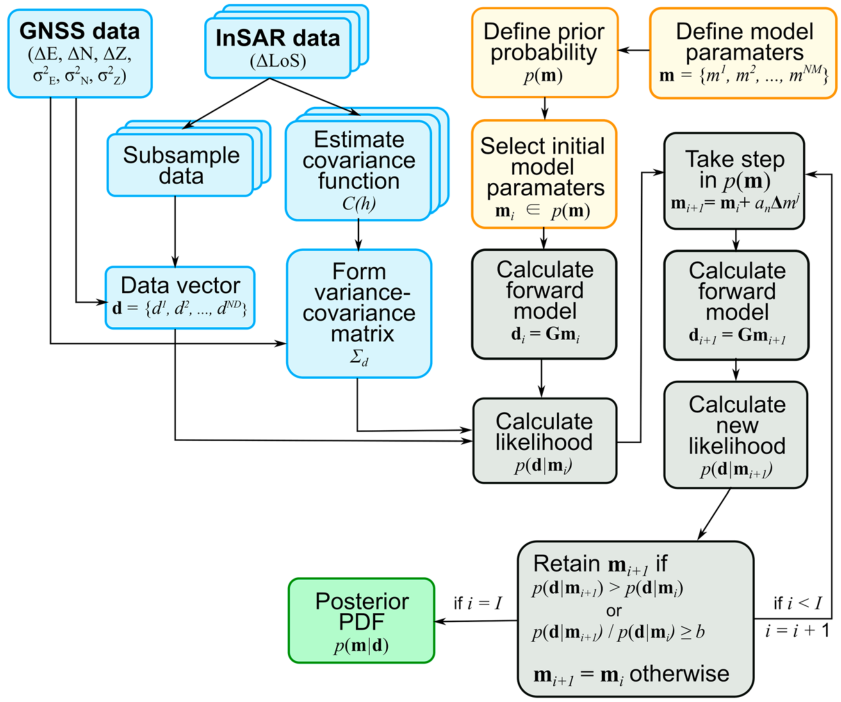

Figure 1. Schematic representation of the proposed Bayesian inversion approach, including the Markov chain Monte Carlo method-Metropolis-Hastings iterative algorithm. Each step is fully described in the text. b is a random value from a uniform distribution within the range [0, 1]. Note that for $i < 20,000$, we perform a sensitivity test (see section 2.2) every N_s iterations to tune the step size Δm^j. GNSS = global navigation satellite system, InSAR = interferometric synthetic aperture radar.

account uncertainties in the data (e.g., data errors and incompleteness) and any available prior information (in the form of a prior PDF). The Bayesian method provides the means to investigate a wealth of statistical inferences, such as point estimates (e.g., mean and median of posterior distributions), credible intervals (e.g., quantiles), and direct probability statements about parameters (e.g., the probability that a certain parameter is greater than a certain value). It also allows analyses of joint and conditional probabilities of pairs or sets of parameters and is particularly instructive in the case of non-Gaussian multimodal posterior PDFs. An optimal set of source parameters can also be extracted from the posterior PDF by finding the maximum a posteriori probability solution.

In this work we propose an approach, summarized in Figure 1, for inverting geodetic data—in particular those derived from InSAR measurements—using a Bayesian probabilistic inversion algorithm capable of including multiple independent data sets (e.g., González et al., 2015; Hooper et al., 2013; Sigmundsson et al., 2014). To efficiently sample the posterior PDFs, we implement a Markov chain Monte Carlo method (MCMC), incorporating the Metropolis-Hastings algorithm (e.g., Hastings, 1970; Mosegaard & Tarantola, 1995), with automatic step size selection. We then review and discuss existing methodologies to characterize errors in InSAR data and to subsample large data sets, which are both necessary steps to be performed prior to an inversion. The proposed method is applied to the inversion of synthetic InSAR and GNSS data to demonstrate the ability of the algorithm to retrieve known source parameters. Finally, as a test case, we invert InSAR data spanning the 2015 M_w 6.4 Pishan (China) earthquake and determine the fault model parameters for this blind thrusting event and validate our results through the comparison with other independent studies (e.g., Ainscoe et al., 2017; He et al., 2016; Wen et al., 2016).

The proposed approach has been implemented in a software package (Geodetic Bayesian Inversion Software [GBIS], http://comet.nerc.ac.uk/gbis) that we make freely available to the scientific community. The software is written in MATLAB® (which is a commercial software and needs to be installed in order to run GBIS) and uses, among others, analytical forward models from the dMODELS software package (Battaglia et al., 2013). Simple mechanical models of crustal deformation that use closed-form analytical solutions for the characterization of magmatically or tectonically induced deformation processes (e.g., Lisowski, 2007; Segall, 2010) can compute surface displacements at 10^3–10^5 observation points in 10^{-3}–10^1 s on consumer-grade computers. These models can be used to place constraints on source location, geometry, orientation, and strength (e.g., volume changes in a magma reservoir and slip on a fault), and their rapidity in computing surface displacements makes them suitable for exploring large numbers (e.g., 10^6) of model parameter combinations. Numerical forward models (e.g., boundary elements method) can also be used to explore more complex source geometries or to take into account complexities in the Earth's crust (e.g., nonflat topographic surface; e.g., Bathke et al., 2015; Cayol & Cornet, 1997; Hooper et al., 2011). However, the increase in complexity in the forward model significantly increases the computational burden, making numerical models less efficient in operational or rapid-response investigations.

Finally, with this work we aim at proposing a detailed guideline for the use of geodetic measurements in inverse problems and present a potential standardized procedure that would allow appropriate comparisons of results obtained by different entities. Inversion results are often used to populate global data sets of deformation source models (e.g., Biggs & Pritchard, 2017; Ebmeier et al., 2018) and should therefore be of comparable quality and obtained with a congruent approach.

2. Bayesian Inversion

For a given discrete inverse problem, the data vector $\mathbf{d} = \{d^1, d^2, \ldots, d^{\mathrm{ND}}\}$ is equal to a nonlinear model function, $\mathbf{G}$, of the model parameters $\mathbf{m} = \{m^1, m^2, \ldots, m^{\mathrm{NM}}\}$, plus error ϵ:

$$\mathbf{d} = \mathbf{G}(\mathbf{m}) + \epsilon \tag{1}$$

In a Bayesian framework, the posterior PDF, $p\,(\mathbf{m}|\mathbf{d})$, describes the probability associated with a given set of model parameters $\mathbf{m}$ that is based on how well such parameters can explain the data $\mathbf{d}$ given their uncertainties, while considering any prior information. The posterior PDF is calculated as follows:

$$p(\mathbf{m}|\mathbf{d}) = \frac{p(\mathbf{d}|\mathbf{m})\,p(\mathbf{m})}{p(\mathbf{d})} \tag{2}$$

where $p(\mathbf{d}|\mathbf{m})$ is the likelihood function of $\mathbf{m}$ given $\mathbf{d}$ based on residuals between the data and the model prediction of the observations, $p(\mathbf{m})$ expresses the prior information (in the form of a prior joint PDF) of the model parameters, and the denominator is a normalizing constant independent of $\mathbf{m}$.

When the errors are multivariate Gaussian with zero mean and covariance matrix Σ_d, $\epsilon \sim N(\mathbf{0}, \Sigma_d)$, the likelihood function is calculated as follows:

$$p(\mathbf{d}|\mathbf{m}) = (2\pi)^{-N/2}|\Sigma_d|^{-\frac{1}{2}}\times \exp\left[-\frac{1}{2}\,(\mathbf{d}-\mathbf{Gm})^{\mathrm{T}}\,\Sigma_d^{-1}\,(\mathbf{d}-\mathbf{Gm})\right] \tag{3}$$

where N is the total number of data points and Σ_d^{-1} is the inverse of the variance-covariance matrix for a given set of data. The data vector $\mathbf{d}$ can be formed from multiple data sets (e.g., multiple SAR interferograms or a combination of interferograms and GNSS data). The likelihood function for multiple data sets, assuming independence, can therefore be expressed as the product of the likelihoods of the data sets (e.g., Fukuda & Johnson, 2008):

$$p(\mathbf{d}|\mathbf{m}) = \Pi_{k=1}^{K}\,(2\pi)^{-N_k/2}|\Sigma_k|^{-\frac{1}{2}}\times\;\exp\left[-\frac{1}{2}\,\mathbf{r}_k^{\mathrm{T}}\,\Sigma_k^{-1}\,\mathbf{r}_k\right] \tag{4}$$

where N_k is the number of data points and $\mathbf{r}_k$ are the residual vectors (difference between observed and modeled data, $\mathbf{r}_k = \mathbf{d}_k - \mathbf{G}_k\mathbf{m}$) associated with each kth data set and K is the total number of data sets. Similarly, the prior probability of the model vector, assuming independence for the model parameters, is the product of the prior probabilities of the different model parameters m^j:

$$p(\mathbf{m}) = \Pi_{j=1}^{NM}p\left(m^j\right) \tag{5}$$

where NM is the total number of model parameters.

Therefore, the Bayesian inversion approach may be preferable in rapid-response or operational settings (e.g., volcano observatories) and in all those cases where fast and robust estimates of source parameters may be needed. If prior probabilities on model parameters are also available, then the Bayesian approach is the only one capable of including these in the inversion. The rapidity of the inversion approach in estimating source parameters, especially in the case of a limited number of GNSS sites (e.g., GNSS data only in the validation example), can also be of use in the planning and design of geodetic monitoring networks. Through the use of synthetic data sets, the effect of a given measurement site can be quantified in terms of its contribution to changes in source parameter uncertainties.

The proposed approach is aimed at the characterization of deformation source parameters through the inversion of static surface displacements spanning a given time interval. While this is of great value for early warning and in the rapid response to events of volcanic unrest and earthquakes, it is not optimized for the study of time-dependent dynamic processes. However, inversion results obtained through our approach are complementary and valuable in instructing other time-variable data assimilation algorithms (e.g., the ensemble Kalman Filter approach for volcano monitoring; Bato et al., 2017; Gregg & Pettijohn, 2016; Zhan & Gregg, 2017). Similarly, the Bayesian approach presented here can instruct or be extended to physical and dynamic models of geodetic and other geophysical measurements, as successfully demonstrated by Anderson and Segall (2013) in the study and forecasting of an episode of volcanic unrest.

Our Bayesian inversion framework aims at being applicable to different geophysical processes, in particular those related to tectonic and magmatic activity, and to both scientific research and natural hazard monitoring. To maintain the flexibility of the algorithm and its ability to efficiently invert different types of geodetic data for a multiplicity of deformation sources, we must rely on certain assumptions and reduce the level of complexity of certain steps. For example, a variety of one- and two-dimensional covariance functions could be applied to characterize errors in InSAR data (e.g., González & Fernández, 2011; Knospe & Jónsson, 2010), or different subsampling methods could be applied to subsample the data (see Section 3.2). While, at this stage, such complexities are not implemented in our approach and in the GBIS software, users can optionally adapt the algorithms to better fit their aims and the desired level of complexity.

7. Conclusions

We have presented a Bayesian approach for the simultaneous inversion of independent geodetic data sets, in particular those from GNSS and InSAR, which takes into account errors in the data and prior information on model parameters. The inversion algorithm, which we implemented in the freely available MATLAB®-based GBIS software, is designed to rapidly estimate optimal model parameters and associated uncertainties through an efficient sampling of the posterior PDFs. Such sampling is performed using a MCMC method incorporating the Metropolis-Hastings algorithm and with an automatic step-size selection. We have applied the inversion method to synthetic GNSS and InSAR data sets and demonstrated its ability to retrieve the true input model parameters. We have also applied the same approach to InSAR data spanning a thrust earthquake and retrieved source parameters for a rectangular fault with uniform slip. Our results are similar to those of previous studies that estimated uncertainties using the added simulated-noise method, but our methodology has been shown to be significantly faster in characterizing optimal model parameters and associated uncertainties, demonstrating its value in rapid-response and operational settings.

Acknowledgments
This work was funded by the NERC Centre for the Observation and Modelling of Earthquakes, Volcanoes and Tectonics (COMET). M. B. and A. H. were both supported by the European Community's Seventh Framework Programme grant 308377 (Project FUTUREVOLC). M. B. was also supported by an appointment to the NASA Postdoctoral Program at the Jet Propulsion Laboratory, administered by the Universities Space and Research Association (USRA) through a contract with NASA. This work was done as a private venture and not in the author's capacity as an employee of the Jet Propulsion Laboratory, California Institute of Technology. Sentinel-1 interferograms were derived from Copernicus SAR data obtained at https://schihub.copernicus.eu. The MATLAB®-based GBIS software can be downloaded from http://comet.nerc.ac.uknerc.ac.uk/gbis together with its user manual and sample synthetic data. MATLAB® is a registered trademark of MatWorks. We acknowledge the helpful comments of the Editor and three anonymous reviewers.

References

Ainscoe, E. A., Elliott, J. R., Copley, A., Craig, T. J., Li, T., Parsons, B. E., & Walker, R. T. (2017). Blind thrusting, surface folding, and the development of geological structure in the M_w6.3 2015 Pishan (China) earthquake. *Journal of Geophysical Research: Solid Earth*, *122*, 9359–9382. https://doi.org/10.1002/2017JB014268

Amey, R. M., Hooper, A., & Walters, R. J. (2018). A Bayesian method for incorporating self-similarity into earthquake slip inversions. *Journal of Geophysical Research: Solid Earth*, *123*. https://doi.org/10.1029/2017JB015316

Anderson, K., & Poland, M. P. (2016). Bayesian estimation of magma supply, storage, and eruption rates using a multiphysical volcano model: Kilauea volcano, 2000–2012. *Earth and Planetary Science Letters*, *447*, 161–171. https://doi.org/10.1016/j.epsl.2016.04.029

Anderson, K., & Segall, P. (2013). Bayesian inversion of data from effusive volcanic eruptions using physics-based models: Application to Mount St. Helens 2004–2008. *Journal of Geophysical Research: Solid Earth*, *118*, 2017–2037. https://doi.org/10.1002/jgrb.50169

Auriac, A., Sigmundsson, F., Hooper, A., Spaans, K. H., Bjornsson, H., et al. (2014). InSAR observations and models of crustal deformation due to a glacial surge in Iceland. *Geophysical Journal International*, *198*(3), 1329–1341. https://doi.org/10.1093/gji/ggu205

Bathke, H., Nikkhoo, M., Holohan, E. P., & Walter, T. R. (2015). Insights into the 3D architecture of an active caldera ring-fault at Tendürek volcano through modeling of geodetic data. *Earth and Planetary Science Letters*, *422*, 157–168. https://doi.org/10.1016/j.epsl.2015.03.041

Bato, M. G., Pinel, V., & Yan, Y. (2017). Assimilation of deformation data for eruption forecasting: Potentiality assessment based on synthetic cases. *Frontiers in Earth Science*, *5*(108), 1–12. https://doi.org/10.3389/feart.2017.00048

Battaglia, M., Cervelli, P. F., & Murray, J. R. (2013). DMODELS: A MATLAB software package for modeling crustal deformation near active faults and volcanic centers. *Journal of Volcanology and Geothermal Research*, *254*(July), 1–4. https://doi.org/10.1016/j.jvolgeores.2012.12.018

Biggs, J., & Pritchard, M. E. (2017). Global volcano monitoring: What does it mean when volcanoes deform? *Elements*, *13*(1), 17–22. https://doi.org/10.2113/gselements

Cayol, V., & Cornet, F. H. (1997). 3D mixed boundary elements for elastostatic deformation field analysis. *International Journal of Rock Mechanics and Mining Science and Geomechanics Abstracts*, *34*(2), 275–287. https://doi.org/10.1016/S0148-9062(96)00035-6

Cervelli, P., Murray, M. H., Segall, P., Aoki, Y., & Kato, T. (2001). Estimating source parameters from deformation data, with an application to the March 1997 earthquake swarm off the Izu Peninsula, Japan. *Journal of Geophysical Research*, *106*(B6), 11,217–11,237. https://doi.org/10.1029/2000JB900399

Currenti, G., Del Negro, C., & Nunnari, G. (2005). Inverse modelling of volcanomagnetic fields using a genetic algorithm technique. *Geophysical Journal International*, *163*(1), 403–418. https://doi.org/10.1111/j.1365-246X.2005.02730.x

Decriem, J., Árnadóttir, T., Hooper, A., Geirsson, H., Sigmundsson, F., Keiding, M., et al. (2010). The 2008 May 29 earthquake doublet in SW Iceland. *Geophysical Journal International*, *181*(2), 1128–1146. https://doi.org/10.1111/j.1365-246X.2010.04565.x

Duputel, Z., Agram, P. S., Simons, M., Minson, S. E., & Beck, J. L. (2014). Accounting for prediction uncertainty when inferring subsurface fault slip. *Geophysical Journal International*, *197*(1), 464–482. https://doi.org/10.1093/gji/ggt517

Ebmeier, S. K., Andrews, B. J., Araya, M. C., Arnold, D. W. D., Biggs, J., Cooper, C., et al. (2018). Synthesis of global satellite observations of magmatic and volcanic deformation: Implications for volcano monitoring and the lateral extent of magmatic domains. *Journal of Applied Volcanology*, *7*(1), 2. https://doi.org/10.1186/s13617-018-0071-3

Elliott, J. R., Walters, R. J., & Wright, T. J. (2016). The role of space-based observation in understanding and responding to active tectonics and earthquakes. *Nature Communications*, *7*, 13844. https://doi.org/10.1038/ncomms13844

Fukuda, J., & Johnson, K. M. (2008). A fully Bayesian inversion for spatial distribution of fault slip with objective smoothing. *Bulletin of the Seismological Society of America*, *98*(3), 1128–1146. https://doi.org/10.1785/0120070194

Fukuda, J., & Johnson, K. M. (2010). Mixed linear-non-linear inversion of crustal deformation data: Bayesian inference of model, weighting and regularization parameters. *Geophysical Journal International*, *181*(3), 1441–1458. https://doi.org/10.1111/j.1365-246X.2010.04564.x

González, P. J., & Fernández, J. (2011). Drought-driven transient aquifer compaction imaged using multitemporal satellite radar interferometry. *Geology*, *39*(6), 551–554. https://doi.org/10.1130/G31900.1

González, P. J., Bagnardi, M., Hooper, A. J., Larsen, Y., Marinkovic, P., Samsonov, S. V., & Wright, T. J. (2015). The 2014–2015 eruption of Fogo volcano: Geodetic modeling of Sentinel-1 TOPS interferometry. *Geophysical Research Letters*, *42*, 9239–9246. https://doi.org/10.1002/2015GL066003

González, P. J., Walters, R. J.; Hatton, E. L., Spaans, K., & Hooper, A. J. (2016). LiCSAR: Tools for automated generation of Sentinel-1 frame interferograms. AGU FAll Meeting.

Gregg, P. M., & Pettijohn, J. C. (2016). A multi-data stream assimilation framework for the assessment of volcanic unrest. *Journal of Volcanology and Geothermal Research*, *309*, 63–77. https://doi.org/10.1016/j.jvolgeores.2015.11.008

Hanssen, R. F. (2001). Radar interferometry data interpretation and error analysis (p. 328). New York: Springer. https://doi.org/10.1007/0-306-47633-9

Hanssen, R. F., Weckwerth, T. M., Zebker, H. A., & Klees, R. (1999). High-resolution water vapor mapping from interferometric radar measurements. *Science*, *283*(5406), 1297–1299. https://doi.org/10.1126/science.283.5406.1297

Hastings, W. K. (1970). Monte Carlo sampling methods using Markov chains and their applications. *Biometrika*, *57*(1), 97–109. https://doi.org/10.1093/biomet/57.1.97

He, P., Wang, Q., Ding, K., Wang, M., Qiao, X., Li, J., et al. (2016). Source model of the 2015 M_w6.4 Pishan earthquake constrained by interferometric synthetic aperture radar and GPS: Insight into blind rupture in the western Kunlun Shan. *Geophysical Research Letters*, *43*, 1511–1519. https://doi.org/10.1002/2015GL067140

Herring, T. A., King, R. W., Floyd, M. A., & McClusky, S. C. (2015). GAMIT reference manual. Release 10.6. Mass. Inst. of Technol. Retrieved from http://geoweb. mit.edu/~simon/gtgk/GAMIT_Ref.pdf

Hooper, A., Ófeigsson, B., Sigmundsson, F., Lund, B., Einarsson, P., Geirsson, H., & Sturkell, E. (2011). Increased capture of magma in the crust promoted by ice-cap retreat in Iceland. *Nature Geoscience*, *4*(11), 783–786. https://doi.org/10.1038/ngeo1269

Hooper, A., Pietrzak, J., Simons, W., Cui, H., Riva, R., Naeije, M., et al. (2013). Importance of horizontal seafloor motion on tsunami height for the 2011 M_w = 9.0 Tohoku-Oki earthquake. *Earth and Planetary Science Letters*, *361*, 469–479. https://doi.org/10.1016/j.epsl.2012.11.013

Hooper, A., Wright, T. J., & Systems, S. (2010). Comparison of Monte Carlo methods for model probability distribution determination in SAR interferometry. *Earth*, *2009*(March), 2–6.

Jeffreys, H. (1939). Theory of probability, Clarendon Press, Oxford. Reprinted in 1961 by Oxford University Press.

Jolivet, R., Simons, M., Agram, P. S., Duputel, Z., & Shen, Z.-K. (2015). Aseismic slip and seismogenic coupling along the central San Andreas fault. *Geophysical Research Letters*, *42*, 297–306. https://doi.org/10.1002/2014GL062222

Jonsson, S. (2002). Fault slip distribution of the 1999 M_w 7.1 Hector Mine, California, earthquake, estimated from satellite radar and GPS measurements. *Bulletin of the Seismological Society of America*, *92*, 1377–1389. https://doi.org/10.1785/0120000922

Juncu, D., Árnadóttir, T., Hooper, A., & Gunnarsson, G. (2017). Anthropogenic and natural ground deformation in the Hengill geothermal area, Iceland. *Journal of Geophysical Research: Solid Earth*, *122*, 692–709. https://doi.org/10.1002/2016JB013626

Knospe, S. H. G., & Jónsson, S. (2010). Covariance estimation for dInSAR surface deformation measurements in the presence of anisotropic atmospheric noise. *IEEE Transactions on Geoscience and Remote Sensing*, *48*(4 PART 2), 2057–2065. https://doi.org/10.1109/TGRS.2009.2033937

Lisowski, M. (2007). Analytical volcano deformation source models. In *Volcano deformation*, (pp. 279–304). Berlin: Springer Praxis Books. Retrieved from papers://8461d6ef-4184−45b2-aa3d-395291ea6525/Paper/p15

Lohman, R. B., & Simons, M. (2005). Some thoughts on the use of InSAR data to constrain models of surface deformation: Noise structure and data downsampling. *Geochemistry, Geophysics, Geosystems*, *6*, Q01007. https://doi.org/10.1029/2004GC000841

McTigue, D. F. (1987). Elastic stress and deformation near a finite spherical magma body: Resolution of the point source paradox. *Journal of Geophysical Research*, *92*(B12), 12931. https://doi.org/10.1029/JB092iB12p12931

Metropolis, N., Rosenbluth, A. W., Rosenbluth, M. N., Teller, A. H., & Teller, E. (1953). Equation of state calculations by fast computing machines. *The Journal of Chemical Physics*, *21*(6), 1087–1092. https://doi.org/10.1063/1.1699114

Minson, S. E., Simons, M., & Beck, J. L. (2013). Bayesian inversion for finite fault earthquake source models I—Theory and algorithm. *Geophysical Journal International*, *194*(3), 1701–1726. https://doi.org/10.1093/gji/ggt180

Mosegaard, K., & Tarantola, A. (1995). Monte Carlo sampling of solutions to inverse problems. *Journal of Geophysical Research*, *100*(B7), 12,431–12,447. https://doi.org/10.1029/94JB03097

Okada, Y. (1985). Surface deformation due to shear and tensile faults in a half-space Okada, Y Bull Seismol Soc AmV75, N4, Aug 1985, P1135–1154. *International Journal of Rock Mechanics and Mining Science and Geomechanics Abstracts*, *75*, 1135–1154. https://doi.org/10.1016/0148-9062(86)90674-1

Pinel, V., Poland, M. P., & Hooper, A. (2014). Volcanology: Lessons learned from synthetic aperture radar imagery. *Journal of Volcanology and Geothermal Research*, *289*, 81–113. https://doi.org/10.1016/j.jvolgeores.2014.10.010

Pritchard, M. E., Simons, M., Rosen, P. A., Hensley, S., & Webb, F. H. (2002). Co-seismic slip from the 1995 July 30 M_w = 8.1 Antofagasta, Chile, earthquake as constrained by InSAR and GPS observations. *Geophysical Journal International*, *150*(2), 362–376. https://doi.org/10.1046/j.1365-246X.2002.01661.x

Roberts, G. O., Gelman, A., & Gilks, W. R. (1997). Weak convergence and optimal scaling of random walk Metropolis algorithms. *Annals of Applied Probability*, *7*(1), 110–120. https://doi.org/10.1214/aoap/1034625254

Roberts, G. O., & Rosenthal, J. S. (2001). Optimal scaling for various Metropolis-Hastings algorithms. *Statistical Science*, *16*(4), 351–367. https://doi.org/10.1214/ss/1015346320

Sahlin, K. (2011). Estimating convergence of Markov chain Monte Carlo simulations. *Annals of Biomedical Engineering*, *32*(9), 1300–1313. Retrieved from http://www.ncbi.nlm. nih.gov/pubmed/15493516

Sambridge, M., & Mosegaard, K. (2002). Monte Carlo methods in geophysical inverse problems. *Reviews of Geophysics*, *40*(3), 1009. https://doi.org/10.1029/2000RG000089

Samsonov, S. V., González, P. J., Tiampo, K. F., & D'Oreye, N. (2014). Modeling of fast ground subsidence observed in southern Saskatchewan (Canada) during 2008–2011. *Natural Hazards and Earth System Sciences*, *14*(2), 247–257. https://doi.org/10.5194/nhess-14-247-2014

Segall, P. (2010). *Earthquake and volcano deformation*. Princeton, NJ: Princeton University Press. https://doi.org/10.1002/0471743984.vse7429

Shirzaei, M., & Walter, T. R. (2009). Randomly iterated search and statistical competency as powerful inversion tools for deformation source modeling: Application to volcano interferometric synthetic aperture radar data. *Journal of Geophysical Research*, *114*, B10401. https://doi.org/10.1029/2008JB006071

Sigmundsson, F., Hooper, A., Hreinsdóttir, S., Vogfjörd, K. S., Ófeigsson, B. G., Heimisson, E. R., et al. (2014). Segmented lateral dyke growth in a rifting event at Bárðarbunga volcanic system, Iceland. *Nature*, *517*(7533), 191–195. https://doi.org/10.1038/nature14111

Simons, M. (2002). Coseismic deformation from the 1999 M_w 7.1 Hector Mine, California, earthquake as inferred from InSAR and GPS observations. *Bulletin of the Seismological Society of America*, *92*(4), 1390–1402. https://doi.org/10.1785/0120000933

Sudhaus, H., & Jónsson, S. (2009). Improved source modelling through combined use of InSAR and GPS under consideration of correlated data errors: Application to the June 2000 Kleifarvatn earthquake, Iceland. *Geophysical Journal International*, *176*(2), 389–404. https://doi.org/10.1111/j.1365-246X.2008.03989.x

Ulrych, T. J., Sacchi, M. D., & Woodbury, A. (2001). A Bayes tour of inversion: A tutorial. *Geophysics*, *66*(1), 55–69. https://doi.org/10.1190/1.1444923

Wackernagel, H. (1995). Variogram and covariance function. In *Multivariate Geostatistics* (pp. 35–40). Berlin: Springer. https://doi.org/10.1007/978-3-662-03098-1_5

Wang, C., Ding, X., Li, Q., & Jiang, M. (2014). Equation-based InSAR data quadtree downsampling for earthquake slip distribution inversion. *IEEE Geoscience and Remote Sensing Letters*, *11*(12), 2060–2064. https://doi.org/10.1109/LGRS.2014.2318775

Wen, Y., Xu, C., Liu, Y., & Jiang, G. (2016). Deformation and source parameters of the 2015 M_w 6.5 earthquake in Pishan, western China, from sentinel-1A and ALOS-2 data. *Remote Sensing*, *8*(2), 1–14. https://doi.org/10.3390/rs8020134

Wright, T. J., Lu, Z., & Wicks, C. (2003). Source model for the M_w 6.7, 23 October 2002, Nenana Mountain earthquake (Alaska) from InSAR. *Geophysical Research Letters*, *30*(18), 1974. https://doi.org/10.1029/2003GL018014

Zhan, Y., & Gregg, P. M. (2017). Data assimilation strategies for volcano geodesy. *Journal of Volcanology and Geothermal Research (special issue on Volcano Geodesy)*, *344*, 13–25. https://doi.org/10.1016/j.jvolgeores.2017.02.015